THE FINITE ELEMENT METHOD IN THE QUANTIFICATION OF THE LOADING SITUATION IN THE HUMAN FEMUR

V.A. Papathanasopoulou, D.I. Fotiadis
and C.V. Massalas

30 – 2001

Preprint, no 30 – 01 / 2001

Department of Computer Science
University of Ioannina
45110 Ioannina, Greece

THE FINITE ELEMENT METHOD IN THE QUANTIFICATION OF THE LOADING SITUATION IN THE HUMAN FEMUR

V.A. Papathanasopoulou
Medical Physics Laboratory,
University of Ioannina, GR 451 10 Ioannina, Greece

D.I. Fotiadis
Dept of Computer Science,
University of Ioannina, GR 451 10 Ioannina, Greece

and
C.V. Massalas
Dept of Materials Science and Engineering,
University of Ioannina, GR 451 10 Ioannina, Greece

1. SUMMARY

In this study, the finite element method (FEM) is employed to describe the strain situation in a model of the human femur under a number of loading conditions. Two three-dimensional models of an intact and an implanted with an endoprosthesis femur are developed. The boundary conditions simulate the instant of peak hip joint contact force in a human femur during the loading cycles of normal walking, up stairs walking, down stairs walking, standing on 2-1-2 legs, and knee bending. The principal surface strain distribution is illustrated in both models and compared. The principal strain values at nodal positions in all aspects of the bone-implant interface are computed in the normal walking situation. The strain values at corresponding positions of the anterior aspect of the interface are compared in all loading conditions. The results can be utilized to indicate the over- and under-loaded areas in an implanted femur in comparison to an intact one, in a variety of loading conditions. A systematic quantification of stresses and strains could prove useful in the understanding of the remodeling process in bone with practical implementation such as in the improvement of endoprosthesis design.

2. INTRODUCTION

The mechanism of load sharing between bone and endoprosthesis is one of the most critical issues in total hip arthroplasty (THA). A change of bone loading after the insertion of an endoprosthesis is expected on local as well as on global level. Higher than normal stresses may lead to fatigue failure of components or disruption of the implant/bone fixation [1]. Reduced stresses due to "stress-shielding" and adaptive bone remodeling may cause bone resorption around femoral hip stems with subsequent loosening, threatening the long-term integrity of the implant [2,3,4]. The study of stress and strain distribution patterns generated by the load-transfer

mechanism and the understanding of their relationships with loading characteristics, prosthetic design, materials, and fixation characteristics, is critical in facing the issue of implant stability. An ideal prosthesis would load the femur in a manner as similar as possible to the natural state. A careful analysis of the stresses in an intact and an implanted bone under a variety of as many realistic-simulating boundary conditions as possible should precede the validation of a certain prosthesis design.

In this paper, the effect of five different loading activities to the load transferred to the femur across a fixed bone-prosthesis interface is studied. These activities include normal walking, up stairs walking, down stairs walking, standing on 2-1-2 legs, and knee bending. The stress and/or strain distribution patterns of the femur and the femur-prosthesis interface during gait and/or arbitrary loading conditions have been extensively studied [6-11], but to our knowledge no comparative study among the five aforementioned activities has been presented. For this purpose, a three-dimensional finite element analysis of an intact and an implanted human femur model is conducted, assuming linear elastic, isotropic and homogeneous material properties. A distinction of the bone material properties in the diaphysis and epiphyses is accounted for. The model is solved quasi-statically, at the instant of peak loading during the loading cycle of each of the activities, employing boundary conditions derived from the literature [12]. The principal surface strain distribution in the intact and the implanted femur models at the instant of peak hip joint reaction force and the maximum and minimum principal strain values at nodal positions along the femoral axis at the bone-implant interface surfaces are computed and compared.

3. MATERIALS AND METHODS

3.1 Intact and implanted model geometry

The geometry of the femur was obtained from the three-dimensional reconstruction of the periosteal contours of 2 mm thickness transverse CT slices of a human cadaver femoral bone. The length of the femur was approximately 350 mm and the diameter of the femoral head was around 40 mm. The femoral head was then removed from the above model and a designed prosthesis was nailed inside the model, simulating a cementless case.

3.2 Material properties

The femur was modelled as a linear elastic, isotropic and homogeneous material. The material properties were distinguished between two principal regions, namely, trabecular bone at the epiphyses and cortical bone in the diaphysis [13] (Table 1). The values of the assigned cortical bone properties are lower than their average values in human cortical femoral bone. This was done in order to compensate for the lack of existence of the medullar canal and the trabecular bone portion present in the diaphysis. The titanium alloy used for the prosthesis material was assumed to be linear elastic, isotropic and homogeneous (Table 1).

3.3 Finite element model

A three-dimensional finite element model was generated using the Patran 8.5 Software (MSC Software Corporation). A solid mesh of the intact femur was constructed consisting of 5584 tetrahedral elements and 1393 nodes. The bone-prosthesis system was meshed with 4593 tetrahedral elements. The contact between bone and the prosthesis was modelled with surface elements. The inner surface of the femoral shaft was meshed with 530 triangular elements, resulting in a total of 5124 elements and 1099 nodes for the bone-implant system, after equivalencing. Friction between bone and the prosthesis was neglected.

Table 1: Material properties for bone and prosthesis.

Property	Cortical Bone [13]	Trabecular Bone [13]	Titanium Alloy [13]
Young's modulus (GPa)	15	0.7	110
Poisson's ratio	0.33	0.2	0.3
Density (kg/m^3)	1650	620	4700

3.4 Boundary conditions and analysis

Five different common activities that cause high hip joint loads were investigated (Table 2) in both an intact and an implanted femur model. The hip-joint reaction force data correspond to the instant of peak hip contact force during the loading cycle, which reflects in mechanical terms a worst case scenario for the behaviour of the bone-implant system. The data were derived from Bergmann *et al.* [12] and are "typical" results calculated with a mathematical averaging procedure from the data of various trials and patients with instrumented hip implants.

A right-handed Cartesian coordinate system with its origin at the center of the femoral head in the intact femur model and a corresponding position in the implanted femur model (Fig. 1) was employed for the definition of the force components acting on the right femur. The +x-axis pointed medially, the +y-axis posteriorly and the +z-axis superiorly. The resultant hip joint reaction force was vectorially applied at a point location on the head of the intact femur model. In the implanted femur model, the resultant force was applied at the corresponding point location on the top of the prosthesis neck. The body weight was taken 75 kg. The distal end of the femur, at the location of the knee joint was constrained in translation and allowed free rotation.

The hip-joint reaction forces were applied quasi-statically to represent the loading cycle. Five runs were done for each of the intact and the implanted femur models, respectively, at the instant of peak hip contact force.

Principal strains were selected to represent the femur load state sufficiently. The principal surface strain distributions in the intact and the implanted femur were compared under the five loading activities. The loading of the implant was assessed by the principal strain values along lines in the bone-implant interface.

The analysis was performed using the Nastran software (Nastran 70.5 MSC Software Corporation) on a Silicon Graphics Origin 2000 Computer (16 CPUs, 3.2 GB Memory).

Table 2: Hip joint reaction force coordinates in five different activities, at the instant of peak hip contact force, in the femur coordinate system [a].

Activity	Peak hip contact force components
Normal walking	[55, 30, 225]
Up stairs	[57, 57, 238]
Down stairs	[58, 40, 250]
Standing on 2-1-2 legs	[30, 12, 224]
Knee bend	[45, 5, 140]

[a] The numbers in the brackets are multipliers of % the body weight (%BW)

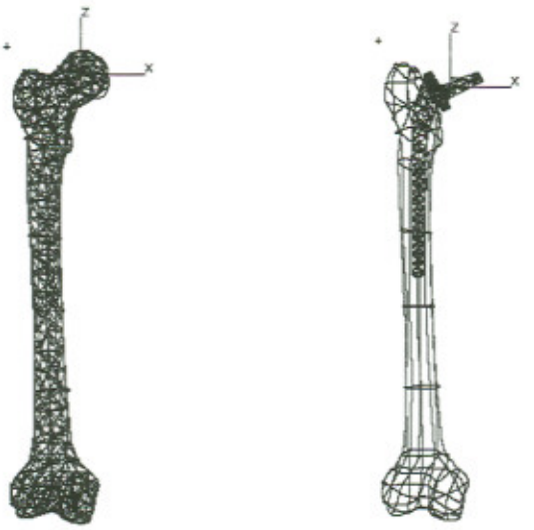

Figure 1: Femur coordinate system in intact and implanted femur models.

4. RESULTS

Fig. 2 illustrates the principal surface strain distribution in the intact femur model at the moment of peak hip contact force during the activities of Table 2. The corresponding distribution in the implanted femur model is shown in Fig. 3. The maximum principal surface strain ranges in both models are tabulated in Table 3. The greatest maximum principal surface strains occur during the up-stairs walking, followed by the down-stairs walking. The lowest maximum principal surface strains occur during knee bend in the intact femur model and during standing on 2-1-2 legs in the implanted one.

The maximum and minimum principal strain values at the medial, lateral, anterior and posterior surfaces of the bone-implant interface during normal walking are plotted in Fig. 4. The points of strain registration correspond to the nodal positions along a line in the superior-inferior direction of the femur at the corresponding surfaces.

The maximum and minimum principal strain values at the anterior surfaces of the bone-implant interface during up stairs walking, down stairs walking, standing on 2-1-2 legs, and knee bend.are shown in Fig. 5.

5. DISCUSSION

The strain and stress distribution and the existence of stress-shielding in implanted femurs have been addressed by several researchers [6-8]. The boundary conditions employed commonly involve the hip joint and muscle forces applied vectorially as point forces during a single or various instances of the gait cycle. The present study focuses on the comparison of the principal strains between an intact and an implanted finite element femur model at the instant of maximum hip joint contact pressure during five different routine activities.

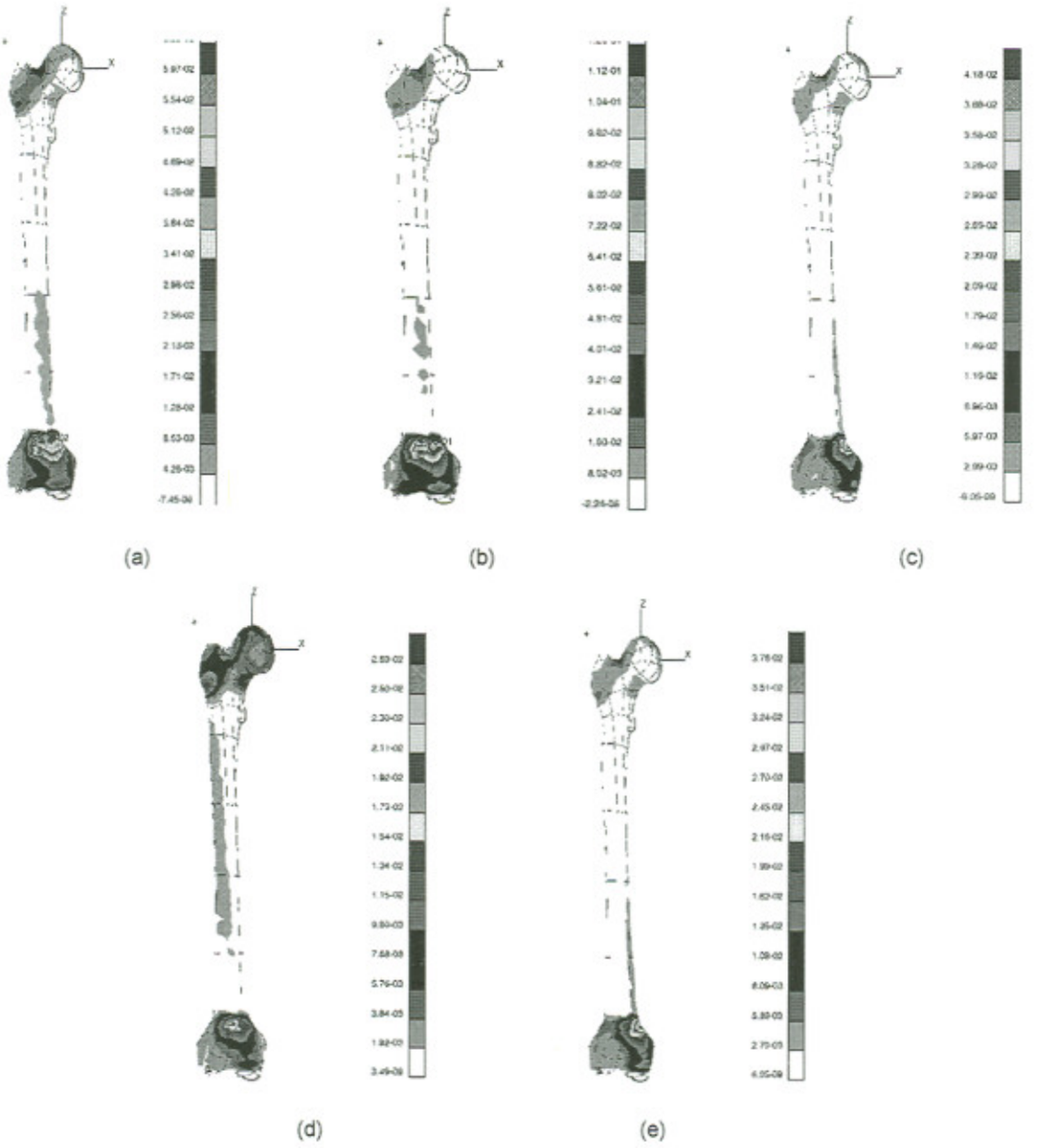

Figure 2: Maximum principal surface strain distribution in the intact femur model at the moment of peak hip contact force during (a) normal walking, (b) up stairs walking, (c) down stairs walking, (d) standing on 2-1-2 legs, and (e) knee bend.

Surface strains

The greatest range of maximum principal surface strains occurs in the up-stairs walking load case in both models.

The surface strains in the intact and the implanted femur models differ by about one order of magnitude, the strains in the implanted femur being lower. This is indicative of the stress-shielding effect in implanted bones.

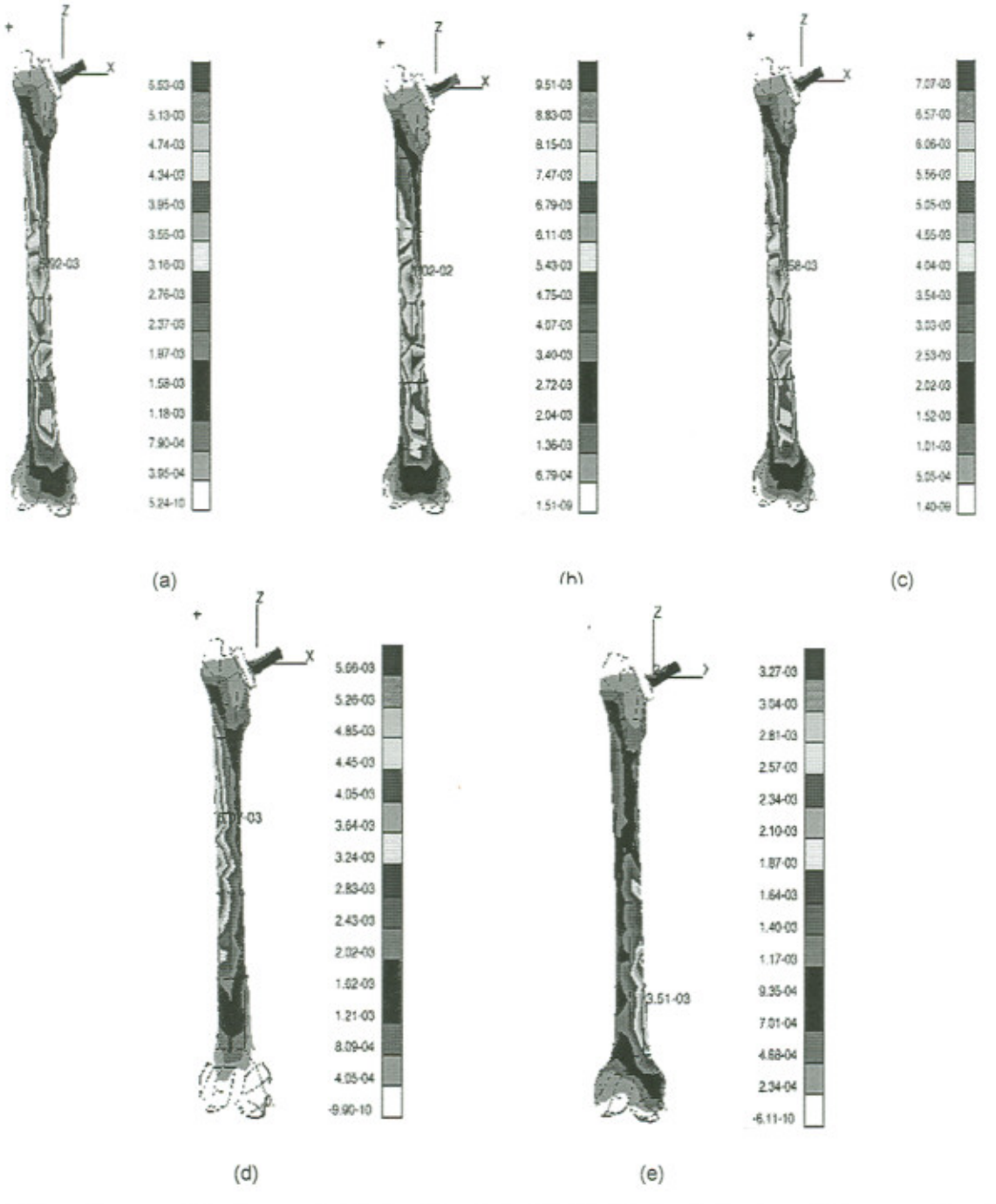

Figure 3: Maximum principal surface strain distribution in the implanted femur model at the moment of peak hip contact force during (a) normal walking, (b) up stairs walking, (c) down stairs walking, (d) standing on 2-1-2 legs, and (e) knee bend.

As shown in Fig. 3, in the implanted femur model the greatest principal surface strains occur on the anterior surface of the femur during normal walking, up stairs walking and down stairs walking. In knee-bending they move towards the medial surface of the mid-lower diaphysis,

Table 3: Maximum principal surface strain ranges in the intact and the implanted femur models.

Activity	Intact femur model	Implanted femur model
Normal walking	4.26×10^{-3} - 6.39×10^{-2}	3.95×10^{-4} - 5.92×10^{-3}
Up stairs	8.02×10^{-3} - 1.20×10^{-1}	6.79×10^{-4} - 1.02×10^{-2}
Down stairs	5.64×10^{-3} - 8.45×10^{-2}	5.05×10^{-4} - 7.58×10^{-3}
Standing on 2-1-2 legs	1.92×10^{-3} - 2.88×10^{-2}	4.05×10^{-4} - 6.07×10^{-3}
Knee bend	2.70×10^{-3} - 4.04×10^{-2}	2.34×10^{-4} - 3.51×10^{-3}

whereas in standing on 2-1-2 legs the greatest strains appear on the lateral surface of the mid-upper diaphysis. Quite different is the situation in the intact femur model. As shown in Fig. 2, the greatest principal surface strains occur on the anterior surface of the lower epiphysis during normal walking, up stairs walking and down stairs walking. In knee bending the maximum strains move to the medial part of the lower epiphysis. In standing on 2-1-2 legs, the region between the femoral head and the greater trochanter experiences the higher strains in addition to the anterior part of the lower epiphysis.

Strains at the bone-implant interface

As shown in Fig. 4, during normal walking, the higher maximum strains occur in the anterior surface of the bone-implant interface, followed by those at the lateral, posterior and medial surfaces.

Anterior strains

The higher maximum and minimum principal strains occur in the up-stairs walking as it is shown in Fig. 5. In general, there is an initial decrease and subsequent increase of the maximum principal strains, when moving from the upper epiphysis towards the diaphysis. The minimum principal strains are nearly constant initially and then they start increasing.

The above findings are qualitatively and quantitatively comparable to those of Duda *et al.* [9], McNamara *et al.* [6], Cristofolini *et al.* [10], and Walker *et al.* [8]. In general, the antero-lateral surfaces of the bone-implant interface are more heavily loaded in comparison to the postero-medial surfaces, at the moment of peak hip joint contact force.

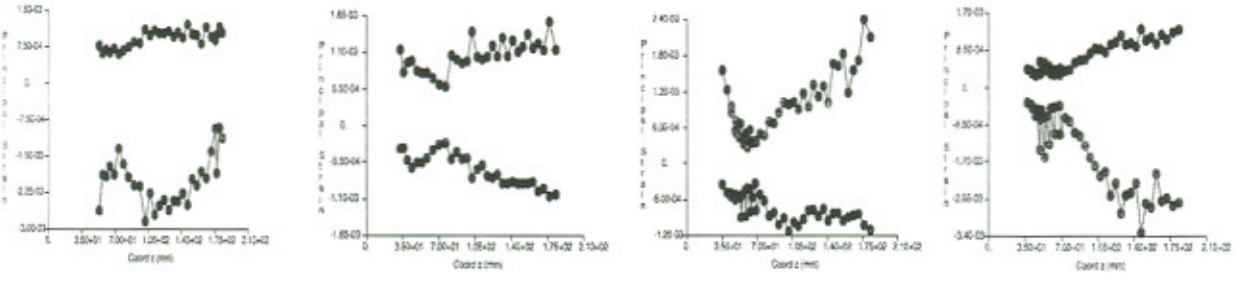

(a) (b) (c) (d)

Figure 4: Maximum (positive) and minimum (negative) principal strain values at the (a) medial, (b) lateral, (c) anterior and (d) posterior surfaces of the bone-implant interface during normal walking. The points in the curves correspond to the node positions along a line in the superior-inferior direction of the femur.

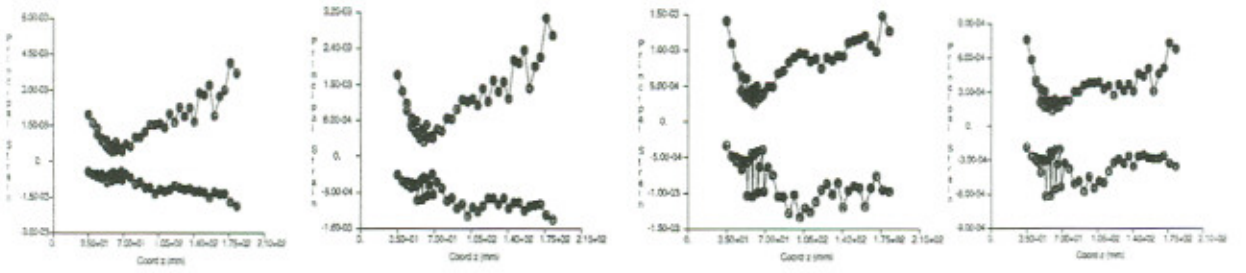

(a) (b) (c) (d)

Figure 5: Maximum (positive) and minimum (negative) principal strain values at the anterior surfaces of the bone-implant interface during (a) up stairs walking, (b) down stairs walking, (c) standing on 2-1-2 legs, and (d) knee bend. The points in the curves correspond to the node positions along a line in the superior-inferior direction of the femur

Stress-shielding is stronger at the transition zone from the upper epiphysis to the diaphysis and becomes less important along the inferior diaphysis.

The present work demonstrates the effectiveness of the three-dimensional finite element method in the mapping of the strain environment in the human femur during a variety of activities. The model can be extended to include other types of loading and instances in the loading cycle. Further work should be undertaken on a model with more realistic constraints such as the inclusion of the various muscle groups acting at different instances of the loading cycle. Verification of such models with experimental data, could potentially lead to the improvement of a particular prosthesis design in relation to the reduction of the stress shielding effect.

6. REFERENCES

[1] R. Huiskes, H. Weinans and M. Dalstra, Adaptive bone remodeling and biomechanical design considerations for noncemented total hip arthroplasty, Orthopedics 12, 1255-1267 (1989).

[2] R. Huiskes, H. Weinans and B. Van Rietbergen, The relationship between stress shielding and bone resorption around total hip stems and the effects of flexible materials, Clinical Orthopedics 272, 124-134 (1992).

[3] A. Toni, B. McNamara, M. Viceconti, A. Sudanese, F. Baruffaldi and A. Giunti, Bone remodelling after total hip arthroplasty, Journal of Materials Science: Materials in Medicine 7, 149-152 (1996).

[4] B. Van Rietbergen, R. Huiskes, H. Weinans and D. R. Sumner, ESB Research Award 1992, The mechanism of bone remodeling and resorption around press-fitted THA stems, Journal of Biomechanics 26, 369-382 (1992).

[5] M. G. Joshi, S. G. Advani, F. Miller and M. H. Santare, Analysis of a femoral hip prosthesis designed to reduce stress shielding, Journal of Biomechanics 33, 1655-1662 (2000).

[6] B. P. McNamara, L. Cristofolini, A. Toni and D. Taylor, Relationship between bone-prosthesis bonding and load transfer in total hip reconstruction, Journal of Biomechanics 30, 621-630 (1997).

[7] L. Cristofolini, A. Cappello, B. P. McNamara and M. Viceconti, A minimal parametric model of the femur to describe axial elastic strain in response to loads, Medical Engineering and Physics 18, 502-514 (1996).

[8] P. S. Walker, D. Schneeweist, S. Murphy and P.Nelson, Strains and micromotions of press-fit femoral stem prostheses, Journal of Biomechanics 20, 693-702 (1987).

[9] G. N. Duda, M. Heller, J. Albinger, O. Schulz, E. Schneider and L. Claes, Influence of muscle forces on femoral strain distribution, Journal of Biomechanics 31, 841-846 (1988).

[10] L. Cristofolini, M. Viceconti, A. Toni and A. Giunti, Influence of thigh muscles on the axial strains in a proximal femur during early stance in gait, Journal of Biomechanics 28, 617-624 (1995).

[11] M. E. Taylor, K. E. Tanner, M. A. R. Freeman and A. L. Yettram, Stress and strain distribution within the intact femur: compression or bending?, Medical Engineering and Physics 18, 122-131 (1996).

[12] G. Bergmann, G. Deuretzbacher, M. Heller, F. Graichen, A. Rohlmann, J. Strauss and G. N. Duda, Hip contact forces and gait patterns from routine activities, Journal of Biomechanics 34, 859-871 (2001).

[13] Y.H. An and R.A. Draughn, Mechanical testing of bone and the bone-implant interface, CRC Press, Boca Raton, FL, USA (2000).

6. DISCUSSION

The strain and stress distribution and the existence of stress-shielding in implanted femurs have been addressed by several researchers [6,7,8]. The boundary conditions employed commonly involve the hip joint and muscle forces applied vectorially as point forces during a single or various instances of the gait cycle. The present study focuses on the comparison of the principal strains between an intact and an implanted finite element femur model at the instant of maximum hip contact pressure during nine different routine activities. The computations verify the presence and compare the intensity of stress shielding in the different loading patterns. A detailed discussion on the principal surface strains in both models and the strains at the bone-implant interface is analytically given below.

Surface strains

The greatest range of maximum principal surface strains occurs in the up-stairs walking load case in both models.

The surface strains in the intact and the implanted femur models differ by about one order of magnitude, the strains in the implanted femur being lower. This is indicative of the stress-shielding effect in implanted bones.

As shown in Fig. 3, in the implanted femur model the greatest principal surface strains occur on the anterior surface of the femur during normal walking, up stairs walking and down stairs walking. In knee-bend they move towards the medial surface of the mid-lower diaphysis, whereas in standing on 2-1-2 legs the greatest strains appear on the lateral surface of the mid-upper diaphysis. Quite different is the situation in the intact femur model. As shown in Fig. 2, the greatest principal surface strains occur on the anterior surface of the lower epiphysis during normal walking, up stairs walking and down stairs walking. In knee bend the maximum strains move to the medial part of the lower epiphysis. In standing on 2-1-2 legs, the region between the femoral head and the greater trochanter experiences the higher strains in addition to the anterior part of the lower epiphysis.

Strains at the bone-implant interface

As shown in Fig. 4, the higher maximum strains occur in the anterior surface of the bone-implant interface, followed by those at the lateral, posterior and medial surfaces.

Anterior strains

The higher maximum and minimum principal strains occur in the up-stairs walking. In general, there is an initial decrease and subsequent increase (at 55 mm) of the maximum principal strains, when moving from the upper epiphysis towards the diaphysis. The minimum principal strains are nearly constant initially and at around 70 mm they start increasing.

The above findings are qualitatively and quantitatively comparable to those of Duda *et al.* [9], McNamara *et al.* [6], Cristofolini *et al.* [10], and Walker *et al.* [8]. Stress-shielding is shown to occur along the entire surface of the intact and implanted models, and is more prominent in the up-stairs loading case, which is also the worst case in terms of loading. The antero-lateral surfaces of the bone-implant interface are more heavily loaded in comparison to the postero-medial surfaces, at the moment of peak hip joint contact force. Stress-shielding is stronger at the

transition zone from the upper epiphysis to the diaphysis and becomes less important along the inferior diaphysis.

The present work shows that three-dimensional finite element analysis is a useful tool in the mapping of the stress-strain environment in the human femur during various activities. The model can be generalised to various types of loading and instances of the gait cycle. Further work should be undertaken on a model with more realistic constraints such as the inclusion of the several different muscle groups applied during different instances of the gait cycle. A verification of such a model with experimental data, could lead to the improvement in the design of intramedullary prostheses in relation to the reduction of the stress shielding effect.